



# A memory-free formulation for determining the non-stationary response of fractional nonlinear oscillators subjected to combined deterministic and stochastic excitations

Renjie Han 

Received: 13 June 2023 / Accepted: 8 October 2023 / Published online: 1 November 2023  
© The Author(s), under exclusive licence to Springer Nature B.V. 2023

**Abstract** A memory-free formulation is proposed for determining the non-stationary stochastic response of fractional single-degree-of-freedom nonlinear/hysteretic dynamic systems subjected to combined periodic and non-stationary stochastic excitations. This is achieved by decomposing the system response in a periodic and a zero-mean stochastic component, while utilizing the memory-free formulation to treat the fractional derivative terms. Specifically, first, the response decomposition leads to a system of coupled differential sub-equations of fractional order governing the deterministic and the stochastic response components. Then, invoking the memory-free formulation, the coupled system of equations is transformed into a system of deterministic and stochastic differential equations with integer-order derivatives. Next, a statistical linearization method-based framework is proposed for treating the stochastic sub-equation. This leads to the determination of the equivalent linear stochastic dynamic system, as well as of the related Lyapunov differential equation. Finally, the Lyapunov differential equation and the deterministic sub-equation with integer-order derivative are solved simultaneously using standard numerical algorithms. The applicability and accuracy of the proposed semi-analytical method is demonstrated by pertinent numerical examples.

**Keywords** Non-stationary stochastic process · Fractional-order derivative · Memory-free formulation · Statistical linearization · Combined excitation

## 1 Introduction

Extensive research has been focused in recent decades on fractional derivative-based modeling of systems in diverse scientific fields, such as physics, applied mathematics and economics [1–4]. In engineering, fractional calculus has been widely used to model the viscoelastic behavior of materials [5–8], since fractional derivative modeling necessitates the use of fewer parameters to achieve better curve fitting of the experimental data both in time and frequency domain. This aspect enables the fractional derivative-based models to capture more efficiently the frequency-dependent force–deformation relationships of viscoelastic/viscous dampers/isolators used for response mitigation of mechanical/structural systems [5,9]. In this regard, theoretical frameworks developed for stochastic response analyses of nonlinear systems with standard derivatives have been extended to account for corresponding systems endowed with fractional derivative elements [10,11]. Further, methods such as stochastic averaging [12,13] and statistical linearization [14–19], as well as path integral-based methods [20,21] have been used successfully for stochastic response determination of fractional-order nonlinear systems. Moreover, based on the orthogonality of the harmonic function and the generalized

---

R. Han (✉)  
College of Civil Engineering, Tongji University, 1239 Siping Road, Shanghai 200092, China  
e-mail: hanrenjie@tongji.edu.cn

harmonic wavelets, a Galerkin method for estimating stationary and non-stationary response spectra of fractional nonlinear systems has been recently developed [22,23].

Clearly, the inherent non-local nature of fractional derivatives potentially leads to computational expensive numerical schemes for determining the system response, e.g., of order  $O(N^2)$ , where  $N$  denotes the number of discrete time steps, especially in long time simulation. In this regard, various solution frameworks have been proposed for improving the computational efficiency of such schemes. These include, for instance, a fixed memory principle [1] and a nested mesh method [24], which can be used to reduce the computational cost to the order of  $O(N \log N)$ . Further, a non-classical memory-free formulation (MFF) was proposed in [25] to transform a system of fractional differential equations with order  $0 < q < 1$  into a system of ordinary differential equations, further reducing in this way the computational cost to the order of  $O(N)$ ; see also [26] and [27] for extensions of the method to account, respectively, for systems with fractional-order  $1 < q < 2$  and with arbitrary non-integer fractional order. Considering the importance of the MFF for performing deterministic system analyses, pertinent MFF-based solution frameworks have been proposed to account for the stochastic response analysis of fractional dynamic systems (e.g., [28,29]). Recently, a novel approach that combines the MFF method with the Wiener path integral technique has been proposed for solving the joint response distribution of fractional-order single-degree-of-freedom systems [30]. An alternative approach, by assuming Gaussian response, has been developed that combines the MFF method with the statistical linearization technique, resulting in significant reduction of computational costs [31,32].

In general, modeling the system excitation as a combined periodic and stochastic action resembles the externally applied load to diverse engineering problems and finds applications such as determining the stationary and non-stationary response of systems spanning from energy-harvesting devices [21,33–35], to slender structures [36,37]. Indicative research on the stationary stochastic response determination of an integer/fractional-order nonlinear/hysteretic system subjected to combined excitations can be found in [30,38–43], and references therein. In addition, considering that the non-stationary excitation potentially includes statistical information of significant importance, a sta-

tistical linearization method for determining the non-stationary stochastic response of integer-order nonlinear systems subjected to combined excitations has been recently proposed in [44]. In this regard, adopting the MFF to treat the derivative terms of fractional order, the method in [44] is extended herein to account for SDOF fractional systems. Specifically, considering that the system response is decomposed into a periodic and a stochastic component leads to a system of coupled fractional-order differential equations governing each one of the components. Then, utilizing the MFF, the fractional-order differential equations are transformed into two (deterministic and stochastic) sets of state-space nonlinear equations [25]. The state-space nonlinear stochastic differential equations (SDEs) are treated by resorting to the statistical linearization method. This leads to a matrix Lyapunov differential equation governing the non-stationary variance/co-variance of the stochastic response vector. Finally, the non-stationary response of the system is determined by jointly treating the state-space deterministic differential equations and the Lyapunov equations. Two numerical examples are used to demonstrate the applicability and the accuracy of the proposed semi-analytical method. These pertain to a Duffing and a Bouc–Wen hysteretic nonlinear oscillators, both endowed with fractional derivative elements and subjected to combined stochastic and periodic excitations. The obtained results are also compared with pertinent Monte Carlo simulation (MCS)-based estimates.

## 2 Mathematical formulation

### 2.1 Equivalent fractional sub-equations of motion

The governing equation of motion of an SDOF nonlinear system endowed with fractional derivative terms and subjected to combined periodic and non-stationary stochastic excitation is given by

$$m\ddot{x}(t) + cD^q x(t) + kx(t) + g(x(t), \dot{x}(t), \ddot{x}(t)) = F(t) + Q(t), \quad (1)$$

where  $x(t)$  denotes the displacement of the system, and  $m$ ,  $c$  and  $k$  are the mass, damping and stiffness coefficients. Further,  $D^q(\cdot)$  represents the Caputo fractional derivative defined as [1]

$$D^q x(t) = \frac{1}{\Gamma(1-q)} \int_0^t \frac{\dot{x}(\tau)}{(t-\tau)^q} d\tau, \quad (2)$$

for fractional-order  $0 < q < 1$ , whereas a dot over a variable denotes differentiation with respect to time.  $g(x(t), \dot{x}(t), \ddot{x}(t))$  is the nonlinear restoring force and

$$Q(t) = a(t)w(t) \tag{3}$$

is a uniformly modulated non-stationary Gaussian process. In Eq. (3),  $a(t)$  represents an amplitude modulating function and  $w(t)$  is a zero-mean stationary white noise process with constant power spectral density  $S_0$ . Further,

$$F(t) = \sum_{l=1}^N f_l \cos(\omega_l t + \theta_l) \tag{4}$$

is a deterministic periodic excitation, in which  $f_l$  represents the amplitude of the  $l$ -th harmonic component with frequency  $\omega_l$  and angle phase  $\theta_l$ , whereas  $N$  denotes the total number of harmonics.

The non-stationary response  $x$  of the system in Eq. (1) can be written as

$$x(t) = \mu_x(t) + \hat{x}(t), \tag{5}$$

where  $\mu_x$  is the deterministic response component and  $\hat{x}$  is the zero-mean stochastic component [42, 43]. Next, differentiating twice with respect to time, as well as applying the fractional-order differentiation on both sides of Eq. (5) yields

$$\begin{aligned} \ddot{x}(t) &= \ddot{\mu}_x(t) + \ddot{\hat{x}}(t), \quad \dot{x}(t) = \dot{\mu}_x(t) + \dot{\hat{x}}(t), \\ D^q x(t) &= D^q \mu_x(t) + D^q \hat{x}(t). \end{aligned} \tag{6}$$

Taking into account the expressions in Eqs. (6), (1) implies

$$\begin{aligned} m \left( \ddot{\mu}_x + \ddot{\hat{x}} \right) + cD^q(\mu_x + \hat{x}) + k(\mu_x + \hat{x}) \\ + g \left( \mu_x + \hat{x}, \dot{\mu}_x + \dot{\hat{x}}, \ddot{\mu}_x + \ddot{\hat{x}} \right) = F(t) + Q(t) \end{aligned} \tag{7}$$

or, equivalently,

$$\begin{aligned} m\ddot{\mu}_x + cD^q(\mu_x) + k\mu_x \\ + E \left[ g \left( \mu_x + \hat{x}, \dot{\mu}_x + \dot{\hat{x}}, \ddot{\mu}_x + \ddot{\hat{x}} \right) \right] = F(t), \end{aligned} \tag{8}$$

where  $E[\cdot]$  represents the mathematical expectation operator. Note, that the interchangeability between the stochastic calculus in the mean squared sense and the expectation is considered for deriving Eq. (8). Subtracting Eq. (8) from Eq. (7) yields the following result:

$$m\ddot{\hat{x}} + cD^q(\hat{x}) + k\hat{x} + h = Q(t), \tag{9}$$

where

$$\begin{aligned} h = g \left( \mu_x + \hat{x}, \dot{\mu}_x + \dot{\hat{x}}, \ddot{\mu}_x + \ddot{\hat{x}} \right) \\ - E \left[ g \left( \mu_x + \hat{x}, \dot{\mu}_x + \dot{\hat{x}}, \ddot{\mu}_x + \ddot{\hat{x}} \right) \right]. \end{aligned} \tag{10}$$

In this context, the original equation of motion is transformed into a set of fractional-order differential sub-equations, which describe the deterministic and stochastic response components as depicted in Eqs. (8) and (9), respectively. Specifically, Eqs. (8) and (9) constitute a set of coupled fractional differential equations to be solved simultaneously for determining the non-stationary response of the system. This is attained in the next section by considering appropriate methods, whose critical characteristic relates to the proper treatment of the fractional derivative elements.

### 2.2 Memory-free formulation of fractional derivatives

The numerical evaluation of the fractional derivative  $D^q x(t)$ , which is defined as the convolution integral in Eq. (2), requires knowledge of the non-local information of the velocity  $\dot{x}(t)$ . Therefore, considering a variable substitution method,  $D^q x(t)$  is transformed into an integral over  $[0, \infty)$ . Specifically, first, the Gamma function is considered

$$\Gamma(q) = \int_0^\infty e^{-s} s^{q-1} ds, \tag{11}$$

where  $\Gamma(q)\Gamma(1-q) = \frac{\pi}{\sin(\pi q)}$ , the fractional derivative in Eq. (2) is reformulated as follows:

$$\begin{aligned} D^q x(t) &= \frac{\sin(\pi q)}{\pi} \int_0^t \left( \int_0^\infty e^{-s} \left( \frac{s}{t-\tau} \right)^q \frac{ds}{s} \right) \dot{x}(\tau) d\tau. \end{aligned} \tag{12}$$

Introducing the new variable  $s = (t - \tau)y^2$ , becomes [45]

$$\begin{aligned} D^q x(t) &= \frac{2 \sin(\pi q)}{\pi} \int_0^\infty y^{2q-1} \left( \int_0^t e^{-(t-\tau)y^2} \dot{x}(\tau) d\tau \right) dy. \end{aligned} \tag{13}$$

Further, defining  $\phi(y, t) = \int_0^t e^{-(t-\tau)y^2} \dot{x}(\tau) d\tau$  and  $b_0 = \frac{2 \sin(\pi q)}{\pi}$ , Eq. (13) is written as

$$D^q x(t) = b_0 \int_0^\infty \phi(y, t) dy. \tag{14}$$

Finally, differentiating the expression for  $\phi(y, t)$  once with respect to time results in the following implication:

$$\dot{\phi}(y, t) = y^{2q-1} \dot{x}(t) - y^2 \phi(y, t). \tag{15}$$

For an in-depth understanding of the MFF, readers are encouraged to refer to [25,46–48] for detailed presentations and practical applications.

Clearly, Eqs. (14) and (15) do not comprise any information about the “past” of the system or, equivalently, no information about the “memory” of  $\dot{x}(t)$  is required. Therefore, Eqs. (14) and (15) represent a MFF corresponding to the fractional derivative definition in the Caputo sense. To solve the memory-free equations numerically, one could approximate the improper integral in Eq. (14) at arbitrarily assigned discrete points  $y_i, i = 1, 2, \dots, n$ . For instance, using the trapezoidal rule [29], Eq. (15) can be cast into a state space form evaluated at  $y_i$ . Then, the resulting  $n$  first-order state-space equations can be solved by adopting any standard numerical method with relevant initial conditions. However, the implementation of this numerical scheme for the MFF is rather computationally expensive, especially since a large number of discrete  $y_i$ 's are required for such a scheme to converge. Nevertheless, extensions of the Gaussian quadrature method, such as the Gauss–Laguerre or the Gauss–Jacob quadrature formulation, can be used to reduce the associated computational cost; see also section “Gauss–Laguerre quadrature-based approximation.”

Therefore, considering Eq. (14), the MFF for the fractional derivatives of the deterministic and the stochastic components of the response (see Eq. 5), is given by

$$\begin{aligned}
 D^q \mu_x(t) &= b_0 \int_0^\infty \phi_1(y, t) dy, \\
 D^q \hat{x}(t) &= b_0 \int_0^\infty \phi_2(y, t) dy,
 \end{aligned}
 \tag{16}$$

where the functions  $\phi_1$  and  $\phi_2$  are defined as

$$\begin{aligned}
 \phi_1(y, t) &= y^{2q-1} \left( \int_0^t e^{-(t-\tau)y^2} \dot{\mu}_x(\tau) d\tau \right), \\
 \phi_2(y, t) &= y^{2q-1} \left( \int_0^t e^{-(t-\tau)y^2} \dot{\hat{x}}(\tau) d\tau \right).
 \end{aligned}
 \tag{17}$$

Then, taking into account the expressions in Eqs. (16), (8) and (9) imply

$$\begin{aligned}
 m\ddot{\mu}_x + cb_0 \int_0^\infty \phi_1(y, t) dy + k\mu_x + E[g(x, \dot{x}, \ddot{x})] \\
 = F(t)
 \end{aligned}
 \tag{18}$$

and

$$m\ddot{\hat{x}} + cb_0 \int_0^\infty \phi_2(y, t) dy + k\hat{x} + h = Q(t),
 \tag{19}$$

respectively. The functions  $\phi_1$  and  $\phi_2$  in Eqs. (18) and (19) satisfy (15), i.e.,

$$\begin{aligned}
 \dot{\phi}_1(y, t) &= y^{2q-1} \dot{\mu}_x(t) - y^2 \phi_1(y, t), \\
 \dot{\phi}_2(y, t) &= y^{2q-1} \dot{\hat{x}}(t) - y^2 \phi_2(y, t),
 \end{aligned}
 \tag{20}$$

and considering Eq. (17), their initial conditions are given by  $\phi_1(y, 0) = \phi_2(y, 0) = 0$ .

Since the evaluation of the fractional-order derivatives depends only on local information of  $\dot{\mu}_x(t)$  and  $\dot{\hat{x}}(t)$ , Eqs. (18) and (19) in conjunction with Eq. (20) represent a MFF of nonlinear/hysteretic SDOF systems endowed with fractional derivative elements defined in the Caputo sense and subjected to combined excitations. Specifically, Eqs. (18–20) define a system of coupled deterministic and stochastic state-space differential equations to be solved simultaneously for determining the system response. This is attained in the ensuing analysis by utilizing appropriate numerical methods. For instance, a brute-force solution which requires sample responses of the state-space differential equations, is obtained by applying the MCS method. As mentioned previously, the improper integrals in Eqs. (18) and (19) can be approximated at arbitrarily assigned discrete points  $y_i, i = 1, 2, \dots, n$ , by using the trapezoidal rule. Then, after casting Eqs. (18–20) into a state space form, any standard numerical scheme can be utilized to solve the resulting  $n + 2$  first-order state-space equations. However, this approach is rather computationally expensive, since a large number of discrete  $y_i$ 's is needed for the method to converge.

### 2.3 Gauss–Laguerre quadrature-based approximation

In this section, an efficient numerical scheme is proposed for approximating the integral in Eq. (18). This is attained by resorting to the Gauss–Laguerre quadrature formula

$$\int_0^\infty f(y, t) dy \approx \sum_{i=1}^n w_i e^{y_i} f(y_i, t),
 \tag{21}$$

where  $w_i$  and  $y_i, i = 1, 2, \dots, n$ , denote, respectively, the Laguerre weights and nodes, and  $f$  is an arbitrary function. Note that the discrete points  $y_i$  used herein are no more arbitrarily chosen.

In this regard, using Eqs. (18), (20) and (21), the deterministic fractional sub-equation of motion shown in Eq. (8) is cast into the state space form

$$\dot{p}_1 = p_2, \tag{22}$$

$$\begin{aligned} \dot{p}_2 = & \frac{F(t)}{m} - \frac{kp_1}{m} - \frac{E[g]}{m} \\ & - \frac{cb_0}{m} \sum_{i=1}^n w_i e^{y_i} \phi_1(y_i, t), \end{aligned} \tag{23}$$

$$\dot{\phi}_1(y_i, t) = y_i^{2q-1} \dot{\mu}_x(t) - y_i^2 \phi_1(y_i, t), \tag{24}$$

for  $i = 1, 2, \dots, n$ , where  $\mathbf{p} = [p_1 \ p_2]^T = [\mu_x \ \dot{\mu}_x]^T$ . Note that  $E[g(x, \dot{x}, \ddot{x})]$  in Eq. (23) depends on the unknown joint probability density function of  $\hat{x}$ ,  $\dot{\hat{x}}$  and  $\ddot{\hat{x}}$ . However, for certain forms of the nonlinear function  $g(x, \dot{x}, \ddot{x})$  and also by considering the Gaussian assumption for the system response [49], a closed-form expression of  $E[g(x, \dot{x}, \ddot{x})]$  is found in terms of the deterministic component and the second moment of stochastic response component; see also in the section ‘‘Numerical examples’’ for the form of the nonlinear function  $g(x, \dot{x}, \ddot{x})$  in case of the Duffing and the Bouc–Wen hysteretic nonlinear oscillators.

Further, additional relationships between the unknowns are needed to supplement the underdetermined system of ordinary differential equations (ODEs) shown in Eqs. (22–24). These are obtained by considering pertinent approximate expressions for the stochastic sub-equations shown in Eqs. (19) and (20). In particular, the utilization of the Gauss–Laguerre quadrature formula presented in Eq. (21), in combination with Eqs. (19) and (20), results in the following set of approximate stochastic differential equations.

$$\begin{aligned} m\ddot{\hat{x}}(t) + cb_0 \sum_{i=1}^n w_i e^{y_i} \phi_2(y_i, t) + k\hat{x}(t) + h \\ = Q(t), \end{aligned} \tag{25}$$

where

$$\begin{aligned} \dot{\phi}_2(y_i, t) = y_i^{2q-1} \dot{\hat{x}}(t) - y_i^2 \phi_2(y_i, t), \\ i = 1, 2, \dots, n. \end{aligned} \tag{26}$$

### 2.4 Statistical linearization for the approximate stochastic differential equations

The statistical linearization is one of the most versatile techniques of random vibration theory for determining the response statistics of nonlinear systems [49,50]. In this section, considering Eqs. (25) and (26), a statistical linearization-based framework is developed to determine the standard deviation of the non-stationary system response.

In this regard, the equivalent linear system of Eq. (25) is written as

$$\begin{aligned} (m + m_e)\ddot{\hat{x}} + cb_0 \sum_{i=1}^n w_i e^{y_i} \phi_2(y_i, t) \\ + c_e \dot{\hat{x}} + (k + k_e)\hat{x} = Q(t), \end{aligned} \tag{27}$$

where

$$m_e = E \left[ \frac{\partial h}{\partial \ddot{\hat{x}}} \right], \quad c_e = E \left[ \frac{\partial h}{\partial \dot{\hat{x}}} \right], \quad k_e = E \left[ \frac{\partial h}{\partial \hat{x}} \right] \tag{28}$$

denote, respectively, the equivalent linear mass, damping and stiffness coefficients, and  $h$  is defined in Eq. (10). Next, Eqs. (26) and (27) are written in the state space form

$$\dot{\mathbf{q}}(t) = \mathbf{G}\mathbf{q}(t) + \mathbf{Q}, \tag{29}$$

where

$$\begin{aligned} \mathbf{q} = [\hat{x} \ \dot{\hat{x}} \ \phi_2(y_1, t) \ \dots \ \phi_2(y_n, t)]^T, \\ \mathbf{Q} = \left[ 0 \ \frac{Q(t)}{m+m_e} \ \dots \ 0 \right]^T \end{aligned} \tag{30}$$

and

$$\mathbf{G} = \begin{bmatrix} 0 & 1 & 0 & \dots & 0 \\ -\frac{k+k_e}{m+m_e} & -\frac{c_e}{m+m_e} & -\frac{a_1 cb_0}{m+m_e} & \dots & -\frac{a_n cb_0}{m+m_e} \\ 0 & y_1^{2q-1} & -y_1^2 & \dots & 0 \\ \vdots & \vdots & \vdots & \ddots & \vdots \\ 0 & y_n^{2q-1} & 0 & \dots & -y_n^2 \end{bmatrix}, \tag{31}$$

with  $a_i = w_i e^{y_i}$ . The Lyapunov equation associated with Eq. (29) for determining the non-stationary covariance matrix is given by

$$\dot{\mathbf{v}} = \mathbf{G}\mathbf{v}^T + \mathbf{v}\mathbf{G}^T + \Theta, \tag{32}$$

where  $\mathbf{v}$  is the covariance matrix of  $\mathbf{q}$ , and  $\Theta$  denotes a  $(n + 2) \times (n + 2)$  matrix whose elements are defined by

$$\theta_{ij} = \begin{cases} \frac{2\pi a^2(t) S_0}{(m+m_e)^2}, & i = j = 2 \\ 0, & \text{otherwise} \end{cases}. \tag{33}$$

### 2.5 Mechanization of the semi-analytical technique

To further elucidate the preceding development, the mechanization of the semi-analytical technique is concisely described in this section. First, note that adopting the Gauss–Laguerre quadrature approximation of Eq. (21) to treat the deterministic sub-equation leads to an underdetermined system of  $n + 2$  nonlinear ODEs

(see Eqs. 22–24). Nevertheless, the Gauss–Laguerre quadrature approximation of the MFF adopted to treat the stochastic sub-equation leads to additional  $n + 2$  nonlinear ODEs (see Eqs. 25–26). For the solution of the system of equations, the proposed semi-analytical technique involves the following steps:

1. Determine the expectation of the nonlinear term  $E[g(x, \dot{x}, \ddot{x})]$  in Eq. (23). Then, obtain the approximate MFF of the deterministic sub-equations in Eqs. (22–24).
2. Determine the equivalent linear parameters  $m_e, c_e$  and  $k_e$  of Eq. (28). Substitute  $m_e, c_e$  and  $k_e$  into Eqs. (31) and (33) to obtain the coefficient matrix  $\mathbf{G}$  and the non-homogeneous matrix  $\Theta$ . Then, construct the Lyapunov equation in Eq. (32).
3. Solve Eqs. (32) and (22–24) simultaneously by applying any standard numerical scheme, such as the Runge–Kutta method, to obtain the deterministic response and the variance/covariance of the stochastic response.

### 3 Numerical examples

In this section, the applicability of the proposed method is demonstrated by considering a Duffing and a Bouc–Wen hysteretic nonlinear oscillators, both endowed with fractional derivative elements and subjected to combined stochastic and periodic excitations.

#### 3.1 Duffing oscillator with fractional derivative terms

The equation of motion of a Duffing oscillator endowed with fractional derivative elements and subjected to combined periodic and non-stationary stochastic excitations is given by

$$m\ddot{x} + cD^q x(t) + kx(1 + \varepsilon x^2) = F(t) + Q(t), \quad (34)$$

where  $g(x(t), \dot{x}(t), \ddot{x}(t)) = \varepsilon kx^3$  is the nonlinear restoring force, with  $\varepsilon > 0$  denoting the nonlinearity magnitude. Further, without loss of generality, the periodic excitation is considered as a monochromatic function, i.e.,  $F(t) = F_0 \sin(\omega_0 t)$ . The non-stationary stochastic excitation is written in a separable form as shown in Eq. (3), with a modulating function

$$a(t) = H(\exp(-\mu_1 t) - \exp(-\mu_2 t)), \quad (35)$$

where the constant  $H$  represents the intensity of the modulating function, and  $\mu_1, \mu_2$  are parameters accounting for its ascent/descent rate.

Next, invoking the Gaussian response assumption, which is often used in the application of the statistical linearization for estimating the statistical moments of nonlinear systems [49], yields

$$E[g(x, \dot{x}, \ddot{x})] = \varepsilon k(3\mu_x \sigma_{\dot{x}}^2 + \mu_x^3), \quad (36)$$

and thus, the equivalent linear parameters defined in Eq. (28) become

$$m_e = 0, \quad c_e = 0, \quad k_e = 3\varepsilon k \left( \sigma_{\dot{x}}^2 + \mu_x^2 \right). \quad (37)$$

Then, the MFF state-space approximation for the deterministic fractional sub-equation is constructed by substituting Eqs. (36) into (22–24). The coefficient matrix  $\mathbf{G}$  and the non-homogeneous matrix  $\Theta$  in the Lyapunov equation are calculated by substituting, respectively, Eqs. (37) and (35) into (31) and (33). Finally, following closely the steps described in the section “Mechanization of the semi-analytical technique,” the response history of the deterministic response component  $\mu_x$  and the standard deviation of the stochastic response component  $v_{11} = \sigma_x$  are obtained.

##### 3.1.1 System response under typical parameters

The following sets of parameters are considered for the numerical implementation:  $m = 1, c = 0.4, k = 1, \varepsilon = 0.1, q = 0.5$  for the system;  $F_0 = 1, \omega_0 = 1$  for the deterministic excitation; and  $H = 1, \mu_1 = 0.1, \mu_2 = 0.2, S_0 = 0.4/\pi$  for the random excitation. Further, the Laguerre node points  $n = 2, n = 4$  and  $n = 8$  are used for Eq. (21), whereas comparisons with pertinent MCS data (10, 000 samples) are used to verify the accuracy of the proposed method. Specifically, the samples of the stochastic excitation used in the Monte Carlo simulation are generated by multiplying the modulating function  $a(t)$  in Eq. (35) by white noise samples synthesized using the spectral representation method [51].

Comparing the results for the system response shown in Fig. 1a and b verifies the accuracy of the proposed method for the resonant situation ( $\omega_0 = \omega_n = 1$ ), where  $\omega_n$  is the natural frequency of the corresponding linear oscillator. Specifically, the deterministic response component and the standard deviation of the stochastic response component obtained

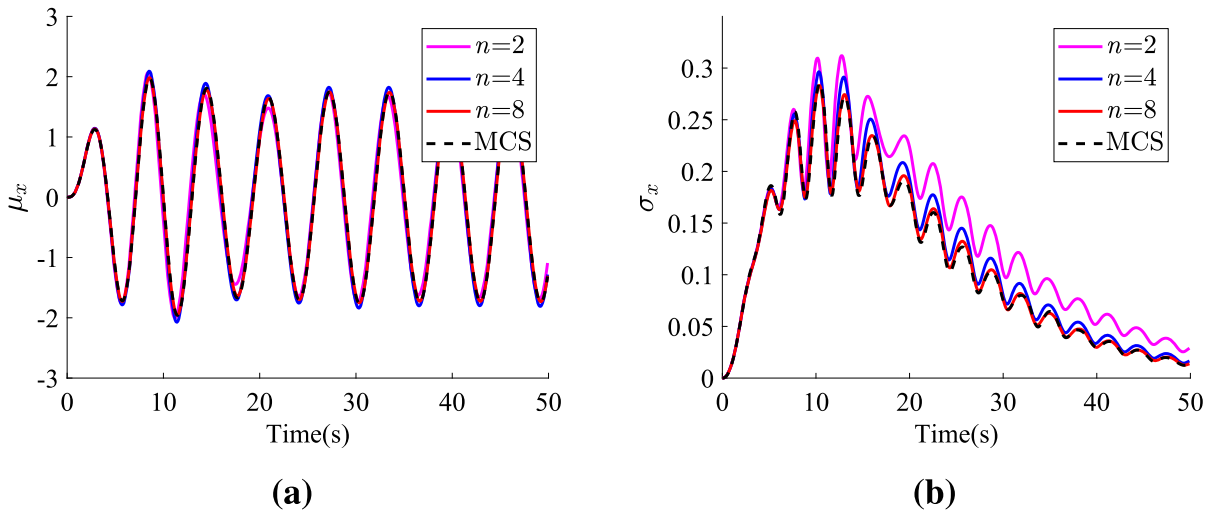


**Fig. 1** Displacement of the fractional Duffing oscillator in Eq. (34) subjected to combined harmonic and stochastic excitations: **(a)** deterministic component and **(b)** standard deviation

of the stochastic component; comparisons with MCS-based estimates (10, 000 samples)

by the proposed method are in satisfactory agreement with the corresponding MCS-based estimates. Besides, the accuracy of the method improves with an increasing value of  $n$ . In this regard, the accuracy attained for the deterministic response is high even when  $n = 2$ , whereas further increasing the value of  $n$  barely improves the accuracy of the results. On the contrary, for the stochastic component standard deviation, the value of  $n$  affects significantly the accuracy of the results obtained by the proposed method. Finally, Fig. 1b shows that the standard deviation obtained by considering that  $n = 8$  agrees perfectly well with the MCS data, which clearly exhibits non-stationarity due to the suddenly applied loading, modulating function and coupling effect with the harmonic excitation.

### 3.1.2 System response parametric analysis

The applicability of the proposed method under various parameters is further investigated in this section. For convenience in comparisons, the time-average modulus (TAM) of the deterministic response is defined as

$$P = \frac{1}{T} \int_0^T \sqrt{\mu_x^2(t)} dt, \tag{38}$$

where  $T$  denotes time duration. Further, the time-averaged standard deviation (TASTD) of the stochastic response component is defined as

$$\bar{\sigma} = \frac{1}{T} \int_0^T \sigma(t) dt. \tag{39}$$

The variation of the TAM of the deterministic response and the TASTD of the stochastic response versus varying nonlinear strength, harmonic excitation amplitude and frequency, and random excitation intensity is investigated in the following. For each case under consideration, all parameters remain the same as those used in the section “System response under typical parameters,” besides the one considered as a varying parameter.

In this regard, first, the applicability of the proposed method for a Duffing oscillator with different levels of nonlinearity is investigated. Figure 2a and b shows, respectively, the TAM of the deterministic response and the TASTD of the stochastic response with varying nonlinearity. It is observed that the accuracy of the proposed method improves with an increasing value of  $n$ . Specifically, Fig. 2a shows that for the TAM, the proposed method yields results with quite high accuracy even when  $n = 2$ , whereas further increasing the value of  $n$  barely improves the accuracy of the method. To the contrary, for the TASTD, the proposed method demonstrates a satisfactory degree of accuracy until  $n = 8$ . Further, both the TAM and the TASTD decrease with increasing the nonlinearity magnitude. Overall, the agreement of the results obtained by the proposed method with the MCS data suggests that the method can

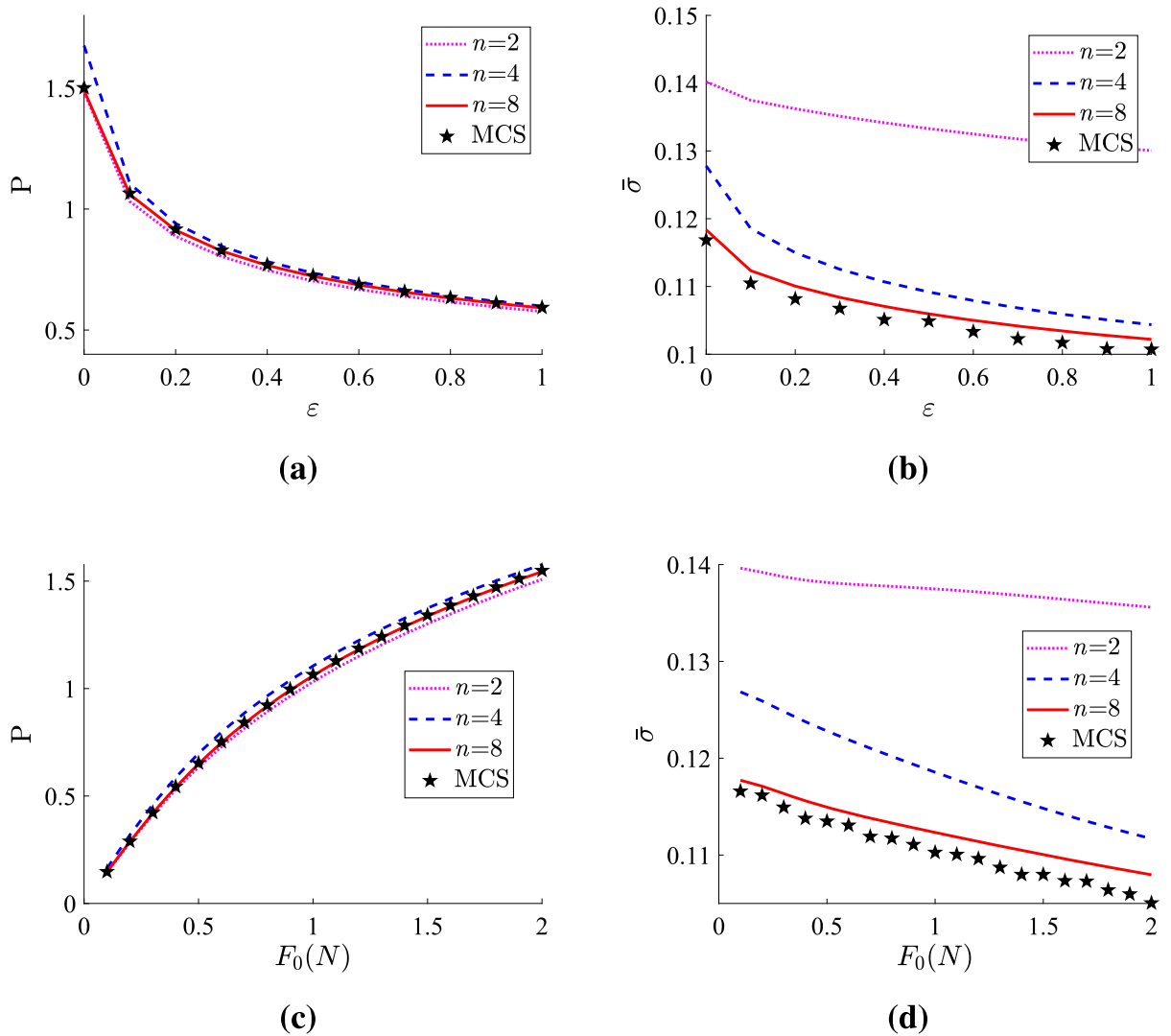


**Fig. 2** Fractional Duffing oscillator in Eq. (34) subjected to combined harmonic and stochastic excitations: (a) TAM of the deterministic response and (b) TASTD of the stochastic response versus nonlinearity; (c) TAM of the deterministic response and

(d) TASTD of the stochastic response versus the deterministic excitation amplitude; comparisons with MCS-based estimates (10, 000 samples)

be readily applied to systems exhibiting strong nonlinearities.

Next, the influence of the harmonic excitation amplitude on the applicability of the proposed method is investigated. Figure 2c and d shows, respectively, the TAM of the deterministic response and the TASTD of the stochastic response, with varying harmonic excitation amplitude. Clearly, the TAM and the TASTD obtained by the proposed method are in satisfactory agreement with the MCS data, demonstrating the appli-

cability of the proposed method when a varying harmonic excitation amplitude is considered. Further, it is seen that with increasing the value of  $n$ , the TASTD converges to the MCS-based estimate faster than the TAM does. Finally, it is clear that with increasing the deterministic excitation frequency, the TAM increases, whereas the TASTD decreases, which indicates a coupling effect between the deterministic and the stochastic components.



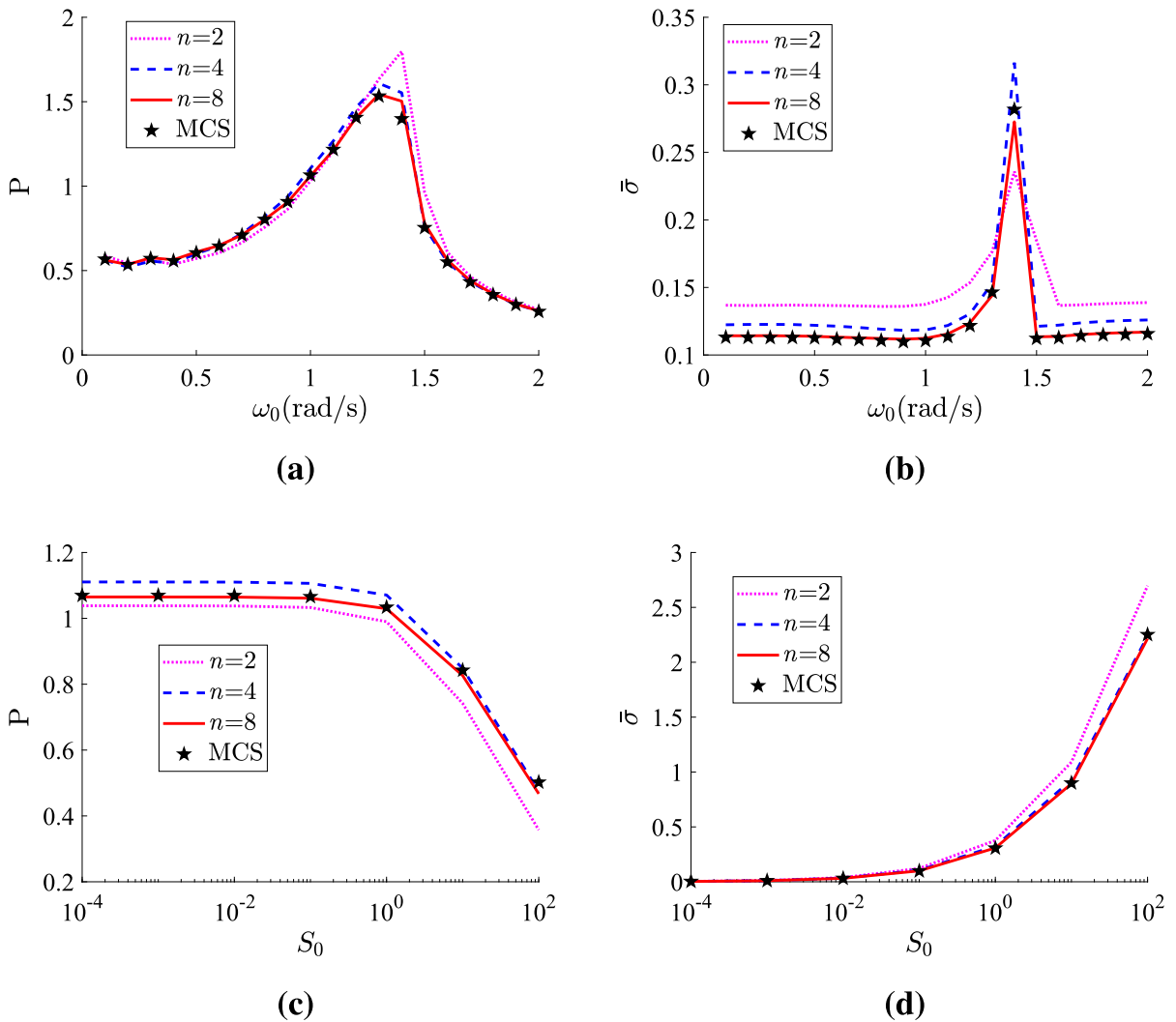


**Fig. 3** Fractional Duffing oscillator in Eq. (34) subjected to combined harmonic and stochastic excitations: (a) TAM of the deterministic response and (b) TASTD of the stochastic response versus harmonic excitation frequency; (c) TAM of the determin-

istic response and (d) TASTD of the stochastic response versus stochastic excitation strength; comparisons with MCS-based estimates (10, 000 samples)

Further, the influence of the harmonic excitation frequency on the applicability of the proposed method is examined. Figure 3a and b shows the TAM and the TASTD versus the harmonic excitation frequency curves of the considered fractional Duffing oscillator subjected to combined excitation. It is readily seen that the TAM and the TASTD obtained by the proposed method are in reasonable agreement with the corresponding MCS data, which demonstrates that the proposed method can be applied for different harmonic excitation frequencies. Moreover, increasing the value

of  $n$  improves rapidly the accuracy of the method, especially for the TASTD of the stochastic response. Next, note that the amplitude–frequency curve shown in Fig. 3a exhibits an asymmetry peak around  $\omega_0 = 1.3$ , which is reasonable since the curve is similar to the amplitude–frequency curve of a hardening Duffing oscillator subjected to harmonic excitation only. Finally, the harmonic excitation frequency has a significant influence on the TASTD of the stochastic response, whose peak value around the resonant frequency  $\omega_0 = 1.3$  is 2–3 times as the values at lower or higher frequen-

cies. This indicates a strong coupling effect between the deterministic and the stochastic components.

Finally, the influence of the stochastic excitation strength  $S_0$ , which varies from  $10^{-4}$  to  $10^2$ , is investigated in the context of the applicability of the proposed method. Figure 3c and d shows, respectively, the TAM of the deterministic response and the TASTD of the stochastic response of the system with varying stochastic excitation strength. The agreement of the results obtained by the proposed method and relevant MCS data improves with an increasing value of  $n$ , demonstrating that the proposed method operates satisfactory well for different levels of stochastic excitation strength. Specifically, the TAM remains almost the same when  $0 < S_0 < 1$  and then decreases dramatically when  $S_0 > 1$ , whereas the TASTD increases rapidly within the entire interval of values considered for  $S_0$ .

### 3.2 Bouc–Wen hysteretic oscillator with fractional derivative terms

In general, models of polynomial nonlinearity cannot completely characterize the hysteretic behavior of materials/components/structures under large deformation. This is due to the hysteretic behavior, which often leads to a force–deformation relationship depending on the entire loading history. In this regard, a Bouc–Wen hysteretic nonlinear oscillator endowed with fractional derivative terms and subjected to combined stochastic and periodic excitations is considered in this example. The system governing equations of motion are written as

$$m\ddot{x}(t) + cD^q x(t) + \varepsilon kx(t) + (1 - \varepsilon)kz(t) = Q(t) + F(t), \tag{40}$$

$$\dot{z}(t) = g_z(\dot{x}, z), \tag{41}$$

where  $\varepsilon$  denotes the rigidity ratio. As an archetypal hysteretic model, the Bouc–Wen hysteretic model captured by the equation [52]

$$\dot{z}(t) = \dot{x}(A - |z|^n (\gamma \operatorname{sgn}(\dot{x}) \operatorname{sgn}(z) + \beta)) \tag{42}$$

is used herein for illustration, where  $A$ ,  $n$ ,  $\gamma$  and  $\beta$  are the Bouc–Wen hysteretic parameters controlling the shape of the hysteresis loops. In particular, when  $n = 1$ , Eq. (42) becomes

$$\dot{z}(t) = A\dot{x} - \gamma z |\dot{x}| - \beta \dot{x} |z|. \tag{43}$$

Further, considering that  $\mathbf{y} = [x \ z]^T$ , Eqs. (40) and (43) are recast in the matrix form

$$m\ddot{\mathbf{y}} + cD^q \mathbf{y} + \mathbf{k}\mathbf{y} + \mathbf{g}(\mathbf{y}, \dot{\mathbf{y}}, \ddot{\mathbf{y}}) = \mathbf{F}(t) + \mathbf{Q}(t), \tag{44}$$

where the parameter matrices are given by

$$\mathbf{m} = \begin{bmatrix} m & 0 \\ 0 & 0 \end{bmatrix}, \quad \mathbf{c} = \begin{bmatrix} c & 0 \\ 0 & 0 \end{bmatrix}, \quad \mathbf{k} = \begin{bmatrix} \varepsilon k & (1 - \varepsilon)k \\ 0 & 0 \end{bmatrix}, \tag{45}$$

the vector of the system nonlinearity has the form

$$\mathbf{g} = \begin{bmatrix} 0 \\ \dot{z} - A\dot{x} + \gamma z |\dot{x}| + \beta \dot{x} |z| \end{bmatrix}, \tag{46}$$

and the deterministic and stochastic excitation vectors are

$$\mathbf{F}(t) = \begin{bmatrix} F(t) \\ 0 \end{bmatrix}, \quad \mathbf{Q}(t) = \begin{bmatrix} Q(t) \\ 0 \end{bmatrix}. \tag{47}$$

Note that, although in this case the equation governing the motion of the fractional oscillator, i.e., Eq. (44), is given in a matrix form, the solution treatment proposed in the section “Mechanization of the semi-analytical technique” is readily applied to obtain the non-stationary response of the considered hysteretic system under combined excitations. Specifically, Eq. (46) yields

$$\mathbf{E}[\mathbf{g}] = \begin{bmatrix} 0 \\ \mu_{\dot{z}} - A\mu_{\dot{x}} + \gamma \mathbf{E}[z |\dot{x}|] + \beta [\dot{x} |z|] \end{bmatrix}, \tag{48}$$

where

$$\begin{aligned} \mathbf{E}[z |\dot{x}|] &= \operatorname{erf}\left(\frac{\mu_{\dot{x}}}{\sqrt{2}\sigma_{\dot{x}}}\right) (\rho_{z\dot{x}}\sigma_z\sigma_{\dot{x}} + \mu_z\mu_{\dot{x}}) \\ &\quad + \sqrt{\frac{2}{\pi}}\mu_z\sigma_{\dot{x}} \exp\left(-\frac{\mu_{\dot{x}}^2}{2\sigma_{\dot{x}}^2}\right) \end{aligned} \tag{49}$$

and

$$\begin{aligned} \mathbf{E}[\dot{x} |z|] &= \operatorname{erf}\left(\frac{\mu_z}{\sqrt{2}\sigma_z}\right) (\rho_{\dot{x}z}\sigma_x\sigma_z + \mu_{\dot{x}}\mu_z) \\ &\quad + \sqrt{\frac{2}{\pi}}\mu_{\dot{x}}\sigma_z \exp\left(-\frac{\mu_z^2}{2\sigma_z^2}\right), \end{aligned} \tag{50}$$

with  $\operatorname{erf}(\cdot)$  denoting the error function. Assuming, next, that the external excitations  $F(t)$  and  $Q(t)$  have the same form with the corresponding excitations considered in the case of the Duffing oscillator (see section “Duffing oscillator with fractional derivative terms”), and adopting the MFF Gauss–Laguerre approximation of Eqs. (21), (22–24) reduce to

$$\dot{p}_1 = p_3, \tag{51}$$

$$\dot{p}_2 = Ap_3 - \gamma E[z|\dot{x}|] - \beta E[\dot{x}|z|], \tag{52}$$

$$\dot{p}_3 = \frac{1}{m} (F_0 \sin(\omega_0 t) - \varepsilon k p_1 - (1 - \varepsilon) k p_2 - c b_0 \sum_{i=1}^n w_i e^{y_i} \phi_1(y_i, t)) \tag{53}$$

and

$$\dot{\phi}_1(y_i, t) = y_i^{2q-1} p_3(t) - y_i^2 \phi_1(y_i, t), \tag{54}$$

where  $\mathbf{p} = [p_1 \ p_2 \ p_3]^T = [\mu_x \ \mu_z \ \mu_{\dot{x}}]^T$ . Further, taking into account the equivalent linear parameters in Eq. (28), the corresponding system equivalent linear matrices are given by

$$\mathbf{m}_e = \mathbf{0}_{2 \times 2}, \quad \mathbf{c}_e = \begin{bmatrix} 0 & 0 \\ -A + \gamma E[z \operatorname{sgn}(\dot{x})] + \beta E[|\dot{x}|] & 0 \end{bmatrix},$$

$$\mathbf{k}_e = \begin{bmatrix} 0 & 0 \\ 0 & \gamma E[|\dot{x}|] + \beta E[\dot{x} \operatorname{sgn}(z)] \end{bmatrix}, \tag{55}$$

where

$$E[z \operatorname{sgn}(\dot{x})] = \sqrt{\frac{2}{\pi}} \rho_{z\dot{x}} \sigma_z \exp\left(-\frac{\mu_{\dot{x}}^2}{2\sigma_{\dot{x}}^2}\right) + \mu_z \operatorname{erf}\left(\frac{\mu_{\dot{x}}}{\sqrt{2}\sigma_{\dot{x}}}\right), \tag{56}$$

$$E[\dot{x} \operatorname{sgn}(z)] = \sqrt{\frac{2}{\pi}} \rho_{\dot{x}z} \sigma_{\dot{x}} \exp\left(-\frac{\mu_z^2}{2\sigma_z^2}\right) + \mu_{\dot{x}} \operatorname{erf}\left(\frac{\mu_z}{\sqrt{2}\sigma_z}\right), \tag{57}$$

$$E(|z|) = \sqrt{\frac{2}{\pi}} \sigma_z \exp\left(-\frac{u_z^2}{2\sigma_z^2}\right) + u_z \operatorname{erf}\left(\frac{u_z}{\sqrt{2}\sigma_z}\right) \tag{58}$$

and

$$E(|\dot{x}|) = \sqrt{\frac{2}{\pi}} \sigma_{\dot{x}} \exp\left(-\frac{u_{\dot{x}}^2}{2\sigma_{\dot{x}}^2}\right) + u_{\dot{x}} \operatorname{erf}\left(\frac{u_{\dot{x}}}{\sqrt{2}\sigma_{\dot{x}}}\right), \tag{59}$$

with  $\operatorname{sgn}(\cdot)$  denoting the signum function. Next, considering Eqs. (30–31) and (33), Lyapunov equation Eq. (32) is formulated, where

$$\mathbf{q} = [\hat{x} \ \hat{z} \ \hat{\dot{x}} \ \phi_2(y_1, t) \ \dots \ \phi_2(y_n, t)]^T,$$

$$\mathbf{Q} = \begin{bmatrix} 0 & \frac{Q(t)}{m} & \dots & 0 & 0 \end{bmatrix}^T, \tag{60}$$

$$\mathbf{G} = \begin{bmatrix} 0 & 0 & 1 & 0 & \dots & 0 \\ 0 & -k_e & -c_e & 0 & \dots & 0 \\ -\frac{\varepsilon k}{m} & \frac{(\varepsilon-1)k}{m} & 0 & -\frac{c b_0 a_1}{m} & \dots & -\frac{c b_0}{a_n} m \\ 0 & 0 & y_1^{2\alpha-1} & -y_1^2 & \dots & 0 \\ \vdots & \vdots & \vdots & \vdots & \ddots & \vdots \\ 0 & 0 & y_n^{2\alpha-1} & 0 & \dots & -y_n^2 \end{bmatrix}, \tag{61}$$

and

$$\theta_{ij} = \begin{cases} \frac{2\pi H^2 (\exp(-\mu_1 t) - \exp(-\mu_2 t))^2 S_0}{m^2}, & i = j = 3 \\ 0, & \text{otherwise} \end{cases} \tag{62}$$

Finally, combining Eqs. (32) with (51–54) and also considering Eqs. (60–62) lead to a system of differential equations, which are solved simultaneously by utilizing a Runge–Kutta numerical scheme.

### 3.2.1 System response under typical parameters

For the numerical implementation of the proposed method, a fractional-order Bouc–Wen hysteretic model is considered, whose system parameters are  $m = 1$ ,  $c = 0.2$ ,  $k = 1$ ,  $\varepsilon = 0.5$ ,  $q = 0.5$ , whereas  $A = 1$ ,  $n = 1$ ,  $\gamma = 0.5$ ,  $\beta = 0.5$  correspond to the softening Bouc–Wen parameters. Further, the deterministic excitation parameters are  $F_0 = 1$ ,  $\omega_0 = 1$ , and the non-stationary stochastic excitation parameters are  $H = 1$ ,  $\mu_1 = 0.1$ ,  $\mu_2 = 0.2$  and  $S_0 = 1$ . Aiming at assessing the relationship between the number of nodes in the MFF Gauss–Laguerre approximation and the accuracy of the proposed method, three separate cases for the number of nodes are considered in the ensuing analysis, namely,  $n = 2$ ,  $n = 4$  and  $n = 8$ . In addition, MCS data (10, 000 samples) are used to verify the accuracy of the method. The samples of non-stationary stochastic excitation are generated by using modulated stochastic samples synthesized by the spectral representation method [51].

The time history of the deterministic response and the standard deviation of the stochastic response for the displacement  $x(t)$ , and the hysteretic displacement  $z(t)$ , are shown in Fig. 4a–d, respectively. Clearly, the results obtained by the proposed method for the system response agree very well with the MCS-based estimates for the resonant case  $\omega_0 = \omega_n = 1$ , where  $\omega_n = \sqrt{\frac{k}{m}}$  is the natural frequency of the corresponding linear system ( $\varepsilon = 1$ ). Moreover, the accuracy of the method is improved with increasing the number of nodes in

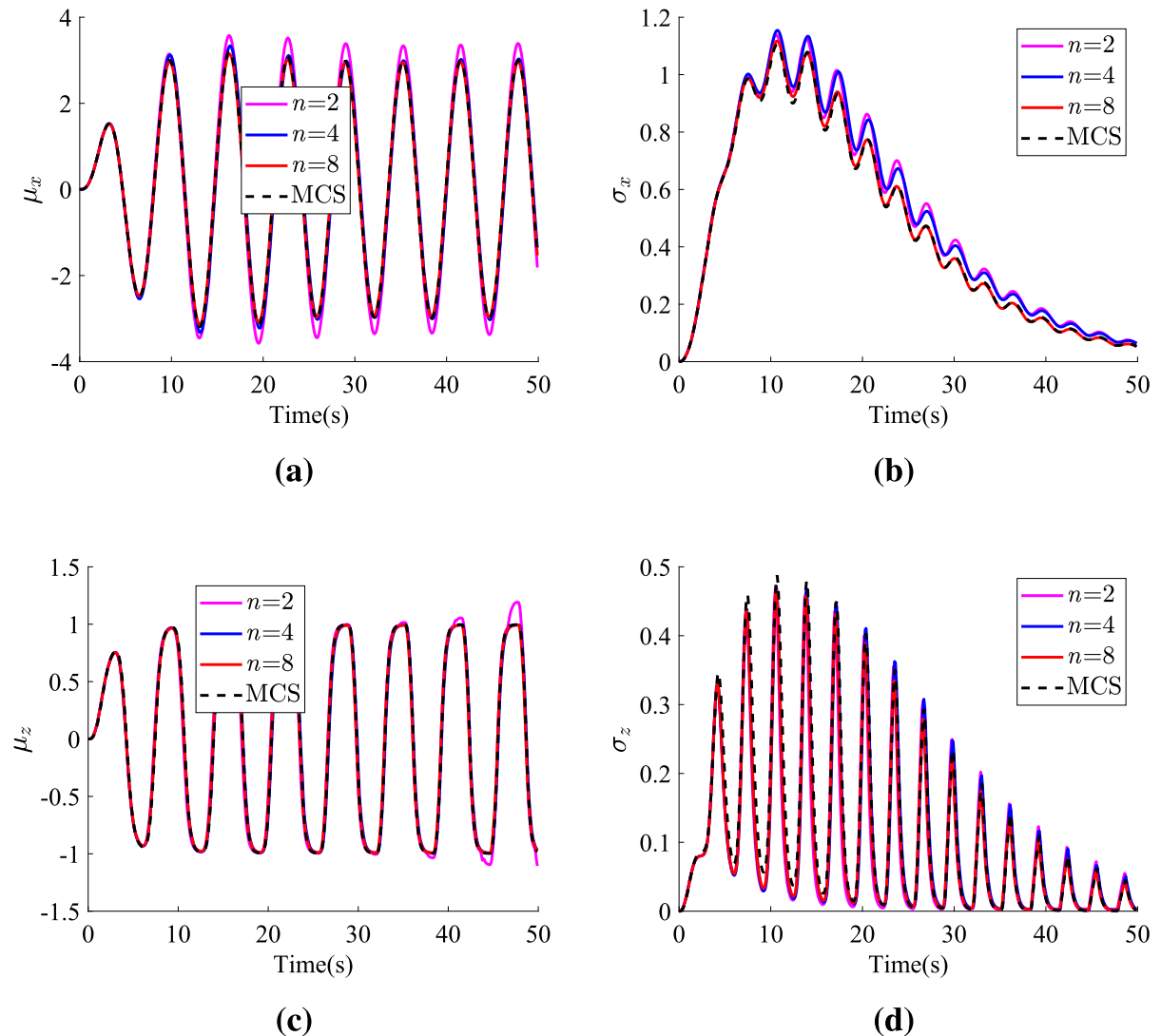


**Fig. 4** Fractional-order Bouc–Wen nonlinear oscillator in Eqs. (40) and (41) subjected to combined harmonic and stochastic excitations: **(a)** deterministic component of the displacement, and **(b)** standard deviation of the stochastic component of the

displacement; **(c)** deterministic component of the hysteretic displacement and **(d)** standard deviation of the stochastic component of the hysteretic displacement; comparison with MCS-based estimates (10,000 samples)

the Gauss–Laguerre approximation. Further, Fig. 4b and d shows that due to the coupling effect between the harmonic and stochastic components, the standard deviations of stochastic responses exhibit harmonic-like oscillations, especially in the decaying phase. In this case, the oscillation amplitude of  $\sigma_z$  is much more intensive than that of  $\sigma_x$ .

### 3.2.2 System response parametric analysis

The applicability of the proposed method for various sets of parameter values is further examined in the ensuing analysis. Specifically, the TAM of the deterministic response and the TASTD of the stochastic response defined, respectively, in Eqs. (38) and (39), are com-

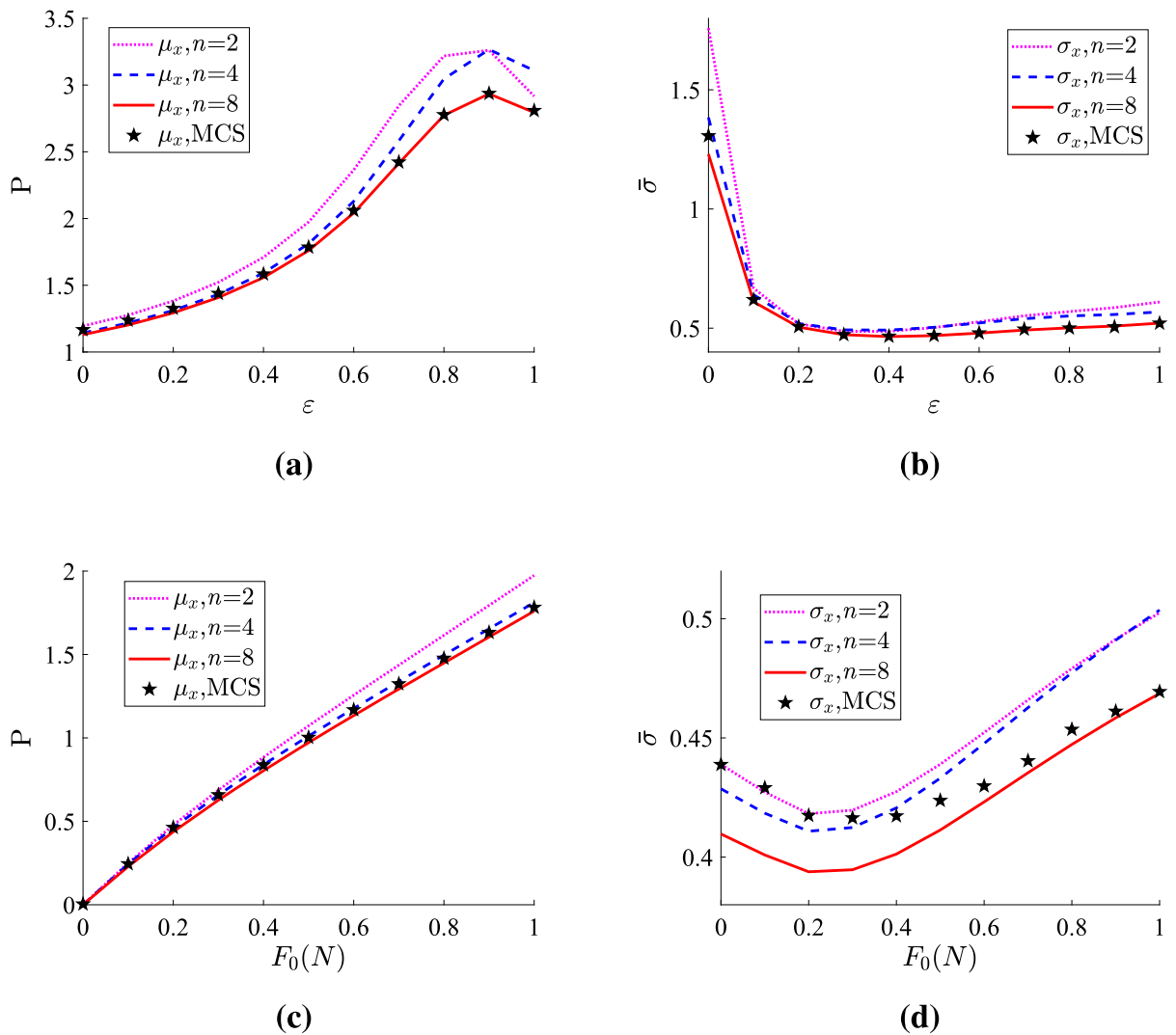


**Fig. 5** Fractional-order Bouc–Wen nonlinear oscillator in Eqs. (40) and (41) subjected to combined harmonic and stochastic excitations: **(a)** TAM of the deterministic response and **(b)** TASTD of the stochastic response versus rigidity ratio; **(c)** TAM

of the deterministic response and **(d)** TASTD of the stochastic component versus the deterministic excitation amplitude; comparison with MCS-based estimates (10,000 samples)

puted for different values of the nonlinear strength, harmonic excitation amplitude and frequency, and stochastic excitation strength. For each one of the considered cases, all parameters remain the same as those used in section “System response under typical parameters,” besides the varying parameters under investigation. The obtained results are compared with pertinent MCS data (10,000 samples).

In this regard, Fig. 5a and b shows, respectively, the TAM of the deterministic response and the TASTD of the stochastic response, with varying rigidity ratio  $\varepsilon$ .

Note that the hysteretic system reduces to the corresponding linear system when  $\varepsilon = 1$ . Clearly, the accuracy of the results calculated by the proposed method, as compared to the MCS-based estimates, improves with increasing the number of node points  $n$ . Further, both the TAM of the deterministic response and the TASTD of the stochastic response do not vary monotonically with the rigidity ratio.

Next, the applicability of the proposed method is investigated in the context of a varying deterministic excitation amplitude. Note that in this case, the system

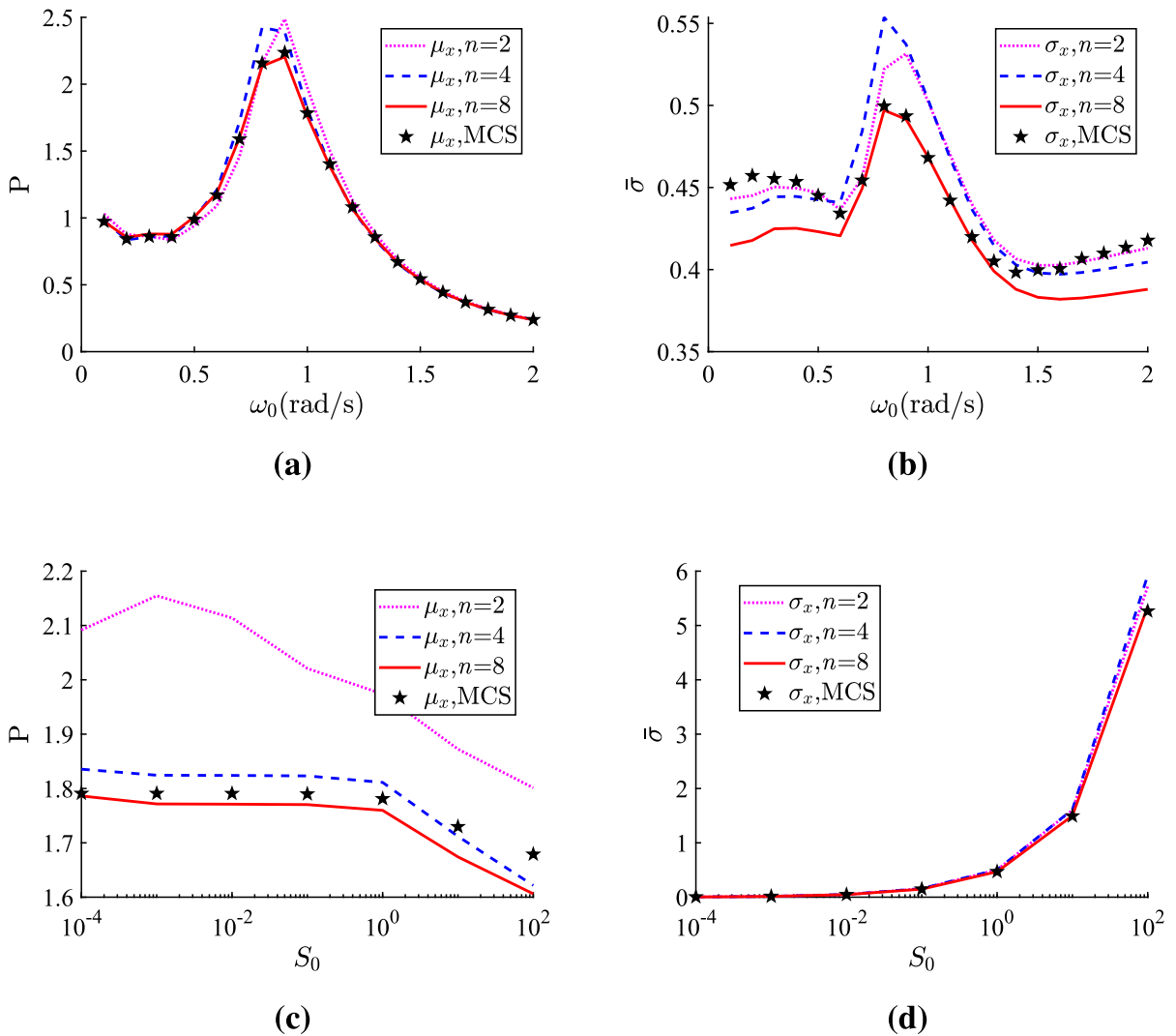


**Fig. 6** Fractional-order Bouc–Wen nonlinear oscillator in Eqs. (40) and (41) subjected to combined harmonic and stochastic excitations: **(a)** TAM of the deterministic response and **(b)** TASTD of the stochastic response versus the deterministic exci-

tation frequency; **(c)** TAM of the deterministic response and **(d)** TASTD of the stochastic response versus the stochastic excitation strength; comparison with MCS-based estimates (10, 000 samples)

reduces to a system subjected to stochastic excitation only when  $F_0 = 0$ . Specifically, Fig. 5c shows that the TAM of the deterministic response increases with increasing  $F_0$ , whereas the TASTD of the stochastic response does not vary monotonically with  $F_0$ , which indicates a coupling effect between the deterministic and the stochastic components. Further, it is seen that the increasing value of  $n$  does not necessarily enhance the accuracy of the proposed method, especially when a low level of deterministic excitation amplitude is considered. Nevertheless, the proposed method exhibits a

satisfactory degree of accuracy, even when  $n = 2$ . The most significant error of the proposed method for the TASTD when  $F_0 = 0$  is less than 10%.

Further, the applicability of the method for different harmonic excitation frequencies is examined. Figure 6a shows the TAM versus  $\omega_0$  curves obtained by the proposed method and the MCS. Clearly, the TAM exhibits an asymmetric peak and shares the same feature as the amplitude–frequency curve of a softening Bouc–Wen system subjected to harmonic excitation. Figure 6b shows the TASTD versus  $\omega_0$  curves obtained

by the proposed method and the MCS. The resonant interval (around  $\omega_0 = 1$ ) of the MCS data exhibits a skew peak, which is predicted by the proposed method when  $n = 8$  with a high degree of accuracy. However, when the excitation frequency is located at the two ends of the considered frequency intervals, the agreement of the results obtained by the proposed method and the MCS-based estimates does not improve with an increasing value of  $n$ .

Finally, the applicability of the proposed method is examined in the context of altering the strength of the stochastic excitation. This is achieved by considering that  $S_0$  takes values in the interval  $[10^{-4}, 10^2]$ . The curves for the TAM of the deterministic response and the TASTD of the stochastic response with varying  $S_0$  are shown in Fig. 6c and d, respectively. Clearly, the accuracy of the proposed method increases with an increasing number of nodes  $n$ . Further, the TAM of the deterministic response almost remains the same when  $0 < S_0 < 1$ , and then decreases rapidly with increasing values of  $S_0$ , whereas the TASTD of the stochastic response increases monotonically with increasing  $S_0$ .

#### 4 Concluding remarks

A semi-analytical technique has been developed for determining the non-stationary response of SDOF nonlinear systems endowed with fractional derivative elements and subjected to combined periodic and non-stationary stochastic excitations. This has been achieved by decomposing the nonlinear equation of motion into a set of fractional-order nonlinear differential equations governing the deterministic and the stochastic response, respectively. Then, combining the Gauss–Laguerre quadrature with a memory-free formulation for fractional derivatives, the fractional-order nonlinear differential equations have been approximated by corresponding nonlinear ODEs and SDEs. Next, a Lyapunov differential equation corresponding to the nonlinear SDEs has been obtained by resorting to the statistical linearization method. Finally, the non-stationary system response has been determined by solving simultaneously the Lyapunov equation and the deterministic ODEs. A critical aspect of the proposed method relates to the number of nodes considered in the Gauss–Laguerre approximation. Specifically, although utilizing more Laguerre nodes has been proved to yield more accurate solutions, as compared to MCS-based

estimates, the method has led to solutions of a satisfactory degree of accuracy even when a relatively small number of Laguerre nodes have been considered.

The validity of the method has been demonstrated by pertinent numerical examples, which have shown its capacity to treat not only fractional SDOF systems exhibiting nonlinear stiffness of the polynomial type, but also systems exhibiting hysteretic behavior. Specifically, a Duffing nonlinear oscillator and a Bouc–Wen hysteretic nonlinear oscillator with fractional derivative terms have been considered. Moreover, a parametric analysis has demonstrated the applicability of the proposed method for a wide range of parameter values. The method can be further extended to systems subjected to combined periodic and non-stationary stochastic excitation described by non-separable power spectral densities.

**Acknowledgements** The corresponding author would like to express his gratitude to professor Fan Kong at Hefei University of Technology and doctor Vasileios C. Fragkoulis at the University of Liverpool for their insightful advice. This work was supported by the National Natural Science Foundation of China (Grant no. 52078399).

**Funding** This work was supported by the National Natural Science Foundation of China (Grant no. 52078399).

**Data availability** All data, models or code that supports the findings of this study is available from the corresponding author upon reasonable request.

#### Declarations

**Competing Interests** The authors declare that they have no known competing financial interests or personal relationships that could have appeared to influence the work reported in this paper.

#### References

1. Podlubny, I.: Fractional differential equations: an introduction to fractional derivatives, fractional differential equations, to methods of their solution and some of their applications. Academic Press, San Diego, CA (1998)
2. Hilfer, R.: Applications of fractional calculus in physics. World Scientific Publishing Co. Pte. Ltd., Singapore (2000)
3. Sabatier, J., Agrawal, O.P., Machado, J.T.: Advances in fractional calculus, vol. 4. Springer (2007)
4. Cai, M., Li, C.: Numerical approaches to fractional integrals and derivatives: a review. *Mathematics* **8**(1), 43 (2020). <https://doi.org/10.3390/math8010043>
5. Makris, N., Constantinou, M.: Spring-viscous damper systems for combined seismic and vibration isolation. *Earthq.*

- Eng. Struct. Dyn. **21**(8), 649–664 (1992). <https://doi.org/10.1002/eqe.4290210801>
6. Rossikhin, Y.A., Shitikova, M.V.: Application of fractional calculus for dynamic problems of solid mechanics: novel trends and recent results. *Appl. Mech. Rev.* **63**(1), 010801 (2009). <https://doi.org/10.1115/1.4000563>
  7. Di Paola, M., Pirrotta, A., Valenza, A.: Visco-elastic behavior through fractional calculus: an easier method for best fitting experimental results. *Mech. Mater.* **43**(12), 799–806 (2011)
  8. Zhang, W., Capilnasiu, A., Sommer, G., Holzapfel, G.A., Nordsletten, D.A.: An efficient and accurate method for modeling nonlinear fractional viscoelastic biomaterials. *Comput. Methods Appl. Mech. Eng.* **362**, 112834 (2020). <https://doi.org/10.1016/j.cma.2020.112834>
  9. Koh, C.G., Kelly, J.M.: Application of fractional derivatives to seismic analysis of base-isolated models. *Earthq. Eng. Struct. Dyn.* **19**(2), 229–241 (1990)
  10. Di Paola, M., Pinnola, F.P., Spanos, P.D.: Analysis of multi-degree-of-freedom systems with fractional derivative elements of rational order. In: ICFDA'14 International Conference on Fractional Differentiation and Its Applications, pp. 1–6. IEEE (2014)
  11. Pirrotta, A., Kougoumtzoglou, I.A., Di Matteo, A., Fragkoulis, V.C., Pantelous, A.A., Adam, C.: Deterministic and random vibration of linear systems with singular parameter matrices and fractional derivative terms. *J. Eng. Mech.* **147**(6), 04021031 (2021)
  12. Chen, L., Wang, W., Li, Z., Zhu, W.: Stationary response of Duffing oscillator with hardening stiffness and fractional derivative. *Int. J. Non-Linear Mech.* **48**, 44–50 (2013). <https://doi.org/10.1016/j.ijnonlinmec.2012.08.001>
  13. Spanos, P.D., Kougoumtzoglou, I.A., dos Santos, K.R.M., Beck, A.T.: Stochastic averaging of nonlinear oscillators: Hilbert transform perspective. *J. Eng. Mech.* **144**(2), 04017173 (2018). [https://doi.org/10.1061/\(asce\)em.1943-7889.0001410](https://doi.org/10.1061/(asce)em.1943-7889.0001410)
  14. Kougoumtzoglou, I.A., Spanos, P.D.: Harmonic wavelets based response evolutionary power spectrum determination of linear and non-linear oscillators with fractional derivative elements. *Int. J. Non-Linear Mech.* **80**, 66–75 (2016). <https://doi.org/10.1016/j.ijnonlinmec.2015.11.010>
  15. Spanos, P.D., Evangelatos, G.I.: Response of a non-linear system with restoring forces governed by fractional derivatives—Time domain simulation and statistical linearization solution. *Soil Dyn. Earthq. Eng.* **30**(9), 811–821 (2010). <https://doi.org/10.1016/j.soildyn.2010.01.013>
  16. Fragkoulis, V.C., Kougoumtzoglou, I.A., Pantelous, A.A., Beer, M.: Non-stationary response statistics of nonlinear oscillators with fractional derivative elements under evolutionary stochastic excitation. *Nonlinear Dyn.* **97**(4), 2291–2303 (2019). <https://doi.org/10.1007/s11071-019-05124-0>
  17. Di Matteo, A., Spanos, P., Pirrotta, A.: Approximate survival probability determination of hysteretic systems with fractional derivative elements. *Probab. Eng. Mech.* **54**, 138–146 (2018). <https://doi.org/10.1016/j.pro bengmech.2017.10.001>
  18. Spanos, P.D., Malara, G.: Nonlinear random vibrations of beams with fractional derivative elements. *J. Eng. Mech.* **140**(9), 04014069 (2014). [https://doi.org/10.1061/\(asce\)em.1943-7889.0000778](https://doi.org/10.1061/(asce)em.1943-7889.0000778)
  19. Spanos, P.D., Di Matteo, A., Cheng, Y., Pirrotta, A., Li, J.: Galerkin scheme-based determination of survival probability of oscillators with fractional derivative elements. *J. Appl. Mech.* **83**(12), 121003 (2016). <https://doi.org/10.1115/1.4034460>
  20. Di Matteo, A., Kougoumtzoglou, I.A., Pirrotta, A., Spanos, P.D., Di Paola, M.: Stochastic response determination of nonlinear oscillators with fractional derivative elements via the wiener path integral. *Probab. Eng. Mech.* **38**, 127–135 (2014). <https://doi.org/10.1016/j.pro bengmech.2014.07.001>
  21. Petromichelakis, I., Psaros, A.F., Kougoumtzoglou, I.A.: Stochastic response analysis and reliability-based design optimization of nonlinear electromechanical energy harvesters with fractional derivative elements. *J. Risk Uncertain. Eng. Syst. Part B: Mech. Eng.* (2021). <https://doi.org/10.1115/1.4049232>
  22. Kong, F., Spanos, P.D.: Response spectral density determination for nonlinear systems endowed with fractional derivatives and subject to colored noise. *Probab. Eng. Mech.* **59**, 103023 (2020)
  23. Kong, F., Zhang, Y., Zhang, Y.: Non-stationary response power spectrum determination of linear/non-linear systems endowed with fractional derivative elements via harmonic wavelet. *Mech. Syst. Signal Process.* **162**, 108024 (2022). <https://doi.org/10.1016/j.ymsp.2021.108024>
  24. Ford, N.J., Simpson, A.C.: The numerical solution of fractional differential equations: speed versus accuracy. *Num. Algorithms* **26**(4), 333–346 (2001). <https://doi.org/10.1023/a:1016601312158>
  25. Yuan, L., Agrawal, O.P.: A numerical scheme for dynamic systems containing fractional derivatives. *J. Vib. Acoust.* **124**(2), 321–324 (2002)
  26. Trinks, C., Ruge, P.: Treatment of dynamic systems with fractional derivatives without evaluating memory-integrals. *Comput. Mech.* **29**(6), 471–476 (2002). <https://doi.org/10.1007/s00466-002-0356-5>
  27. Diethelm, K.: An investigation of some nonclassical methods for the numerical approximation of caputo-type fractional derivatives. *Num. Algorithms* **47**(4), 361–390 (2008). <https://doi.org/10.1007/s11075-008-9193-8>
  28. Di Paola, M., Failla, G., Pirrotta, A.: Stationary and non-stationary stochastic response of linear fractional viscoelastic systems. *Probab. Eng. Mech.* **28**, 85–90 (2012). <https://doi.org/10.1016/j.pro bengmech.2011.08.017>
  29. Failla, G., Pirrotta, A.: On the stochastic response of a fractionally-damped duffing oscillator. *Commun. Nonlinear Sci. Numer. Simul.* **17**(12), 5131–5142 (2012). <https://doi.org/10.1016/j.cnsns.2012.03.033>
  30. Zhang, Y., Kougoumtzoglou, I.A., Kong, F.: A wiener path integral technique for determining the stochastic response of nonlinear oscillators with fractional derivative elements: a constrained variational formulation with free boundaries. *Prob. Eng. Mech.* **71**, 103410 (2023). <https://doi.org/10.1016/j.pro bengmech.2022.103410>
  31. Spanos, P.D., Zhang, W.: Nonstationary stochastic response determination of nonlinear oscillators endowed with fractional derivatives. *Int. J. Non-Linear Mech.* **146**, 104170 (2022). <https://doi.org/10.1016/j.ijnonlinmec.2022.104170>
  32. Zhang, W., Spanos, P.D., Di Matteo, A.: Nonstationary stochastic response of hysteretic systems endowed with frac-



- tional derivative elements. *J. Appl. Mech.* **90**(6), 061011 (2023). <https://doi.org/10.1115/1.4056946>
33. Dai, Q., Harne, R.L.: Investigation of direct current power delivery from nonlinear vibration energy harvesters under combined harmonic and stochastic excitations. *J. Intell. Mater. Syst. Struct.* **29**(4), 514–529 (2018)
  34. Cai, W., Harne, R.L.: Characterization of challenges in asymmetric nonlinear vibration energy harvesters subjected to realistic excitation. *J. Sound Vib.* **482**, 115460 (2020)
  35. Pasparakis, G.D., Kougioumtzoglou, I.A., Fragkoulis, V.C., Kong, F., Beer, M.: Excitation-response relationships for linear structural systems with singular parameter matrices: a periodized harmonic wavelet perspective. *Mech. Syst. Signal Process.* **169**, 108701 (2022)
  36. Davenport, A.: The response of slender structures to wind. In: *Wind Climate in Cities*, pp. 209–239. Springer (1995)
  37. Tessari, R.K., Kroetz, H.M., Beck, A.T.: Performance-based design of steel towers subject to wind action. *Eng. Struct.* **143**, 549–557 (2017)
  38. Spanos, P.D., Zhang, Y., Kong, F.: Formulation of statistical linearization for m-d-o-f systems subject to combined periodic and stochastic excitations. *J. Appl. Mech.* **86**(10), 101003 (2019). <https://doi.org/10.1115/1.4044087>
  39. Zhang, Y., Spanos, P.D.: Efficient response determination of a M-D-O-F gear model subject to combined periodic and stochastic excitations. *Int. J. Non-Linear Mech.* **120**, 103378 (2020). <https://doi.org/10.1016/j.ijnonlinmec.2019.103378>
  40. Zhang, Y., Spanos, P.D.: A linearization scheme for vibrations due to combined deterministic and stochastic loads. *Probab. Eng. Mech.* **60**, 103028 (2020). <https://doi.org/10.1016/j.probengmech.2020.103028>
  41. Kong, F., Spanos, P.D.: Stochastic response of hysteresis system under combined periodic and stochastic excitation via the statistical linearization method. *J. Appl. Mech.* **88**(5), 1–12 (2021)
  42. Ni, P., Fragkoulis, V.C., Kong, F., Mitseas, I.P., Beer, M.: Response determination of nonlinear systems with singular matrices subject to combined stochastic and deterministic excitations. *ASCE-ASME J. Risk Uncertain. Eng. Syst. Part A: Civ. Eng.* **7**(4), 04021049 (2021). <https://doi.org/10.1061/ajrua6.0001167>
  43. Kong, F., Han, R., Zhang, Y.: Approximate stochastic response of hysteretic system with fractional element and subjected to combined stochastic and periodic excitation. *Nonlinear Dyn.* (2021). <https://doi.org/10.1007/s11071-021-07014-w>
  44. Kong, F., Han, R., Li, S., He, W.: Non-stationary approximate response of non-linear multi-degree-of-freedom systems subjected to combined periodic and stochastic excitation. *Mech. Syst. Signal Process.* **166**, 108420 (2022). <https://doi.org/10.1016/j.ymsp.2021.108420>
  45. Schmidt, A., Gaul, L.: On a critique of a numerical scheme for the calculation of fractionally damped dynamical systems. *Mech. Res. Commun.* **33**(1), 99–107 (2006). <https://doi.org/10.1016/j.mechrescom.2005.02.018>
  46. Diethelm, K.: An improvement of a nonclassical numerical method for the computation of fractional derivatives. *J. Vib. Acoust.* **131**(1), 014502 (2009). <https://doi.org/10.1115/1.2981167>
  47. Birk, C., Song, C.: An improved non-classical method for the solution of fractional differential equations. *Comput. Mech.* **46**(5), 721–734 (2010). <https://doi.org/10.1007/s00466-010-0510-4>
  48. Liu, Q.X., Chen, Y.M., Liu, J.K.: An improved Yuan-Agrawal method with rapid convergence rate for fractional differential equations. *Comput. Mech.* **63**(4), 713–723 (2018). <https://doi.org/10.1007/s00466-018-1621-6>
  49. Roberts, J.B., Spanos, P.D.: *Random vibration and statistical linearization*. Courier Corporation (2003)
  50. Kougioumtzoglou, I.A., Fragkoulis, V.C., Pantelous, A.A., Pirrotta, A.: Random vibration of linear and nonlinear structural systems with singular matrices: a frequency domain approach. *J. Sound Vib.* **404**, 84–101 (2017). <https://doi.org/10.1016/j.jsv.2017.05.038>
  51. Shinozuka, M., Deodatis, G.: Simulation of stochastic processes by spectral representation. *Appl. Mech. Rev.* **44**(4), 191–204 (1991). <https://doi.org/10.1115/1.3119501>
  52. Ismail, M., Ikhouane, F., Rodellar, J.: The hysteresis Bouc-Wen model, a survey. *Archiv. Comput. Methods Eng.* **16**(2), 161–188 (2009)

**Publisher's Note** Springer Nature remains neutral with regard to jurisdictional claims in published maps and institutional affiliations.

Springer Nature or its licensor (e.g. a society or other partner) holds exclusive rights to this article under a publishing agreement with the author(s) or other rightsholder(s); author self-archiving of the accepted manuscript version of this article is solely governed by the terms of such publishing agreement and applicable law.